Structure, Volume *20*

Supplemental Information

An Asymmetry-to-Symmetry Switch in Signal Transmission by the Histidine Kinase Receptor for TMAO

Jason O. Moore and Wayne A. Hendrickson

Inventory of Supplemental Information

SUPPLEMENTAY MATERIALS AND METHODS

Cloning, Expression and Purification for Biophysical Studies

$vpTorS_S$

Cloning, expression, and purification of $vpTorS_S$ (residues 51 – 319 plus a residual N-terminal GSGS after thrombin cleavage) were described previously (Moore & Hendrickson, 2009).

vpTorT

A DNA fragment corresponding to most of mature TorT (secreted residues 29 to 329 of 334) was amplified from genomic DNA of *V. parahaemolyticus EB10* using 5' and 3' primers containing BamHI and Xho1 restriction sites respectively with a stop codon engineered immediately following the last residue of the construct. The fragment was ligated into the pETDuet-t expression vector between the BamHI and Xho1 sites of the polylinker region. The resulting construct was used for isopropyl-β-D-thiogalactopyranoside (IPTG)-inducible cytoplasmic expression of vpTorT as a fusion protein, containing a hexahistidine tag on the N-terminus separated by a thrombin protease recognition sequence. A residual N-terminal GSGS cleavage sequence remains, as for $vpTorS_S$, which we treat in coordinate files as mutated variants.

vpTorT was expressed in Novagen *E. coli* Origami2(DE3) cells, grown in 8L of LB media at 37°C to an optical density (OD) of 0.6, after being inoculated 1:100 from an overnight culture grown in LB media. Expression was induced using IPTG at 0.25 mM overnight at 20°C after incubation for 20 minutes on ice and the addition of ethanol to 1% final concentration. The cells were harvested and resuspended in 50mM Tris-HCl pH 8.0 and 200mM NaCl. Cell supernatant was prepared by sonication, cleared by centrifugation, and then passed through a 5ml HiTrap™ Chelating column (Pharmacia) previously equilibrated with Ni^{2+}. The protein was eluted from the column using an imidazole gradient. The eluate was dialyzed against 50mM Tris-HCl pH 8.0 and 200mM NaCl and subsequently digested with thrombin (1U thrombin/mg protein) overnight at 20°C. The digested protein was again passed through a 5ml HiTrap™ Chelating column (Pharmacia) previously equilibrated with Ni^{2+}. The protein that was successfully digested with thrombin did not bind the column and was collected.

Thrombin-cleaved vpTorT protein was further purified by gel filtration on a Superdex75 26/60 (Pharmacia) column, previously equilibrated in 50mM Tris-HCl pH 8.0 and 200mM NaCl. Protein eluted as a single band corresponding to 35 kDa. At this point, two populations of protein were identified: the full-length protein (33820 Da) and a cleavage product (31420 Da), which by N-terminal sequencing is only C-terminally truncated. Accordingly, the corresponding recombinant protein, $TorT_{\Delta C}$ with C-terminal Lys308, was produced in an analogous manner. Native gel (8-25% polyacrylamide gradient) electrophoresis shows that $TorT_{\Delta C}$ is not identical with the TorT cleavage product; instead, it has a mobility corresponding to net charge -2 rather than -1 (Fig. S3).

$vpTorS_S$-vpTorT Complex

On native PAGE it appeared that the full-length vpTorT was able to bind $vpTorS_S$ while the thrombin cleavage product was not. The proteins were therefore mixed with an approximately molar equivalent amount of $vpTorS_S$ and further purified on a Superdex75 26/60 column previously equilibrated in 50mM Tris-HCl pH 8.0 and 200mM NaCl. The eluate that contained both $vpTorS_S$ and vpTorT was collected and dialyzed against 10mM Tris pH 8.0, 25mM NaCl and was concentrated to a final concentration of 30mg/mL for crystallization.

$vpTorS_S$-$vpTorS_S$

To generate a protein that consists of two $TorS_S$ molecules fused by a flexible 25-residue linker ($vpTorS_S$-$TorS_S$), the sequence corresponding to residues 51 to 323 of TorS ($vpTorS_S$) was amplified from genomic DNA of *V. parahaemolyticus EB101* into two DNA fragments, one flanked by BamHI and EcoRI restriction enzyme sites and the other flanked by NotI and Xho restriction enzyme sites. The two fragments were then sequentially inserted between the BamHI and EcoRI restriction enzyme sites and the NotI and XhoI restriction enzyme sites of pETDuetT. A linker comprising alternating codons for glycine and serine residues and flanked by EcoRI and NotI restriction sites was then inserted between the EcoRI and NotI sites to yield a 25-residue linker sequence of $LN(SG)_{10}A_3$ between the $TorS_S$ segments. Expression, and purification of $vpTorS_S$-$vpTorS_S$ (plus a residual N-terminal GSGS after thrombin cleavage) was performed as per $vpTorS_S$.

Crystallization

Three crystal forms of the vpTorS_S-vpTorTp complex were identified and used in structure solution. In each case a protein concentration of 30 mg/ml was used.

Crystals of the first form were grown at 4°C by hanging drop vapor diffusion against a buffer containing 4-7% isopropanol, 0.9-1.4M NH_4 citrate pH 6.5 with a protein to reservoir buffer ratio of 2:1. Clusters of large single needles appeared after a few days. The crystals were soaked in buffer solution supplemented with 28% ethylene glycol prior to freezing in liquid nitrogen.

For the second crystal form, TMAO from a 5M stock was added to the protein solution to a final concentration of 5mM before crystallization. Crystals were grown at 4°C by hanging drop vapor diffusion against a buffer containing 0.4-0.8M Ca acetate, 4-7% butanol, 0.1M MES pH 6.0-6.5 with a protein to reservoir buffer ratio of 3:1. Clusters of large cube-shaped crystals appeared after a few days. The crystals were soaked in buffer solution supplemented with 30% glycerol prior to freezing in liquid nitrogen.

Crystals of the third form were grown at 4°C by hanging drop vapor diffusion against a buffer containing 1-4% PEG 400, 1.0-1.7M $(NH_4)_2SO_4$, 100 mM Tris pH 8.0 with a protein to reservoir buffer ratio of 3:1. Large prismatic crystals grew after a few days. The crystals were soaked in buffer solution supplemented with 25% ethylene glycol prior to freezing in liquid nitrogen.

Structure Determination

SeMet vpTorS_S-TorT in complex with isopropanol

MAD data from four wavelengths at the Se K-edge were collected from a single frozen SeMet Para TorS_S crystal at the X4C beamline of the NSLS at Brookhaven National Labs. Data to 3.0Å spacings (275mm detector distance) were collected using 1° oscillations of 25.4s exposure times. The data were indexed and merged using Denzo and Scalepack of the HKL program package (Otwinowski & Minor, 1997). Initial phases were calculated using Solve (Terwilliger & Berendzen, 1999) and improved by solvent flattening using DM (Cowtan, 1994) of the CCP4 program package (Bailey, 1994). A figure of merit of 0.36 was obtained from phasing and refinement of six selenium sites found in the two molecules of the asymmetric unit, and after solvent flattening, the figure of merit rose to 0.904. Diffraction data are shown in Table S1.

vpTorS$_S$-TorT in complex with isopropanol

A native dataset to 3Å spacings (230mm detector distance) from a single frozen crystal was collected at X4C of the NSLS at Brookhaven National Labs using 0.5° oscillations with 45.4s exposure times. The data was indexed, merged, and processed using the HKL program package (Otwinowski & Minor, 1997) and the CCP4 program suite (Bailey, 1994) in space group $P2_12_12_1$. Phases obtained from SeMet vpTorSS-TorT were extended to 3Å spacings using DM (Cowtan, 1994). The previously solved structure of TorS$_S$ was fit into density using O and this initial model was refined with CNS. An initial model for TorT was then built using Arp/Warp 6.0 (Perrakis et al, 1999) that only consisted of helical fragments. Using these fragments as a guide the two domains from the structure of the maltose binding protein were independently fit into density. The model was then refined in CNS (Brunger et al, 1998) using iterative cycles of simulated annealing, conjugate gradient minimization, temperature-factor refinement, and manual rebuilding with O. Diffraction data are in Table S1, refinement statistics are in Table 1, and the PDB id is 3O1J.

vpTorS$_S$-TorT in complex with TMAO

A native dataset to 3.1Å spacings (500mm detector distance) from a single frozen crystal was collected at 14-BM-C of the APS at Argonne National Laboratory using 0.75° oscillations with 20s exposure times. Because of high error factors in the low resolution data only data to 8.0Å was used and a low resolution dataset was collected from the same crystal to 3.5Å spacings (500mm detector distance) using 1° oscillations of 20s exposure times. The data was indexed, merged, and processed using the HKL program package (Otwinowski & Minor, 1997) and the CCP4 program suite (Bailey, 1994) in space group $C222_1$. Phases were obtained using Phaser. A solution was obtained used one copy each of the TorS$_S$ and TorT structures from the vpTorS$_S$-TorT in complex with isopropanol. The initial model was put through a single round of rigid body refinement using Refmac. The model was then refined in CNS (Brunger et al, 1998) using iterative cycles of simulated annealing, conjugate gradient minimization, temperature-factor refinement, and manual rebuilding with O. Diffraction data are in Table S1 and refinement statistics are in Table 1, and the PDB id is 3O1H.

vpTorS$_S$-TorT apo

A native dataset to 2.8Å spacings (217mm detector distance) from a single frozen crystal was collected at X4C of the NSLS at Brookhaven National Labs using 0.5° oscillations with 14.2s exposure times. The data was indexed, merged, and processed using the HKL program package (Otwinowski & Minor, 1997) and the CCP4 program suite (Bailey, 1994) in space group $C222_1$. Phases were obtained using Phaser. A solution was obtained using the complete homotetramer from the vpTorS$_S$-TorT in complex with isopropanol. The initial model was put through a single round of rigid body refinement using Refmac. The model was then refined in CNS (Brunger et al, 1998) using iterative cycles of simulated annealing, conjugate gradient minimization, temperature-factor refinement, and manual rebuilding with O. Diffraction data are in Table S1 and refinement statistics are in Table 1, and the PDB id is 3O1I. PDB chain identifications are TorS' (A), TorS'' (B), TorT'(D), and TorT''(C).

Analytical Ultracentrifugation

A Beckman/Coulter XLI analytical ultracentrifuge with absorbance optics was used for sedimentation equilibrium experiments. Purified vpTorS$_S$TorS$_S$ and vpTorT were concentrated until the two proteins were each about 1.5 mg/mL, 1 mg/mL and 0.5mg/mL. Samples were loaded into three channels of a six channel cell with sapphire windows and a path length of ~1.2mm with a buffer blank in the other channels. This same procedure was performed with samples in the presence of 10 mM TMAO. Both experiments were performed in duplicate. All samples were sedimented to equilibrium in an AN-50 Ti rotor spun at 10000, 13000, and 16000 rpm at 20°C with absorbance scans taken at one hour intervals. The program WinMatch (written by J. Lary & D. A. Yphantis, University of Connecticut) was used to verify the attainment of equilibrium. Equilibrium data from all three speeds were fit as a group using HeteroAnalysis (v 1.0.104 written by J. Cole and J. Lary, University of Connecticut).

Isothermal Titration Calorimetry

Measurements were carried out at 20° C in a buffer of 50 mM Tris pH 8.0, 200 mM NaCl on a VP ITC (GEHealthcare, Microcal, Northhampton, MA) with 30 μM vpTorS$_S$TorS$_S$-vpTorT complex in the cell and 1.2 mM TMAO in the syringe. An initial 2 μl injection was followed by 10 injections of 3 μl and another 50 injections of 5 μl at 240 second intervals.

Heat of dilution was computed from the last ten injections and subtracted from the raw data. Data analysis was performed by Origin 7.0.

Cell Strains and Cloning for Analyses of Cellular Activity

All of the bacterial strains used in the β-galactosidase assays were generated starting from strain N7723 (genotype N99 *lacZX*A21), which the Gottesman lab generously provided to us from their collection. To generate *torS-torT* deficient cells N7723 cells carrying the pSIM4 vector were prepared following a described protocol (Datta et al, 2006). Electroporation of a PCR product containing the chloramphenicol marker from pACYC184 flanked by 50 base pairs homologous to the first 50 5' to 3' base pairs of TorS on the 5' end and the last 50 3' to 5' base pairs of TorT on the 3' end. The transformed cells were streaked onto LB agar plates with 10 μg/mL chloramphenicol and grown overnight at 37°C. Colonies were picked and checked for the removal of the *torT-torS* locus using PCR and subsequent sequencing of the PCR product. A colony so identified is labeled strain N7723ΔTS.

Removal of the *pcnB* gene was accomplished using P1 transduction as described in Silhavy (Silhavy et al, 1984). Removal of the *pcnB* gene was checked using PCR and subsequent sequencing of the PCR product. The strain so generated is labeled N7723ΔTS-pCN.

The *lacZ* gene from the pBAD/*Myc*-His/*lacZ* plasmid (bases 373-3429), was amplified using 5' and 3' primers containing NcoI and XhoI restriction sites respectively and was inserted between the NcoI and XhoI sites of pBAD/*Myc*-His B. The 186 base pairs upstream of the *torCAD* operon regulatory region from the genomic DNA of *E. coli K-12* (ATCC Bioproducts) which contains the regulated tor boxes was amplified using 5' and 3' primers containing BamHI and NcoI sites respectively and was subsequently inserted between the BamHI and NcoI sites. This plasmid is labeled pCAD-*lacZ*.

The *torT-torS* loci from the genomic DNA of *E. coli K-12* was amplified using 5' and 3' primers containing XhoI and XbaI restriction sites respectively and inserted between the XhoI and XbaI sites in pCAD-*lacZ*. This plasmid is labeled pCAD-*lacZ*/TS. Mutations in pCAD-*lacZ*/TS were generated using a described protocol (Wang & Malcolm, 2002).

To generate the Tar and NarX chimeras it was necessary to first make conserved mutations resulting in BglII sites centered in residues 343 and 389 and NheI sites centered in residues 350 and 401 of TorS. The chimeras were then generated by amplifying the appropriate fragments of NarX or Tar from the genomic DNA of *E. coli K-12* flanked by the appropriate restriction enzyme sites and inserted between the KpnI site upstream of the TorS start site and the appropriate BglII or NheI site that was generated earlier.

β-Galactosidase Assay

All strains, except for those that contain a chimera vectors, were grown in LB media with 10 μg/mL of ampicillin overnight at 37°C. Following a 1:1000 dilution into 5 mL tube filled with of LB media with 10 μg/mL of ampicillin and the appropriate concentration of TMAO. The tubes were then capped, leaving little air in the tube, and grown for five hours at 37°C. The β-galactosidase activity was the measured using the Pierce Biotechnologies β-Galactosidase assay kit. All assays were performed in triplicate from separate cultures.

The same procedure was performed on strains that contained chimera vectors except MOPS minimal media (Neidhardt et al, 1974) was used instead of LB, and the appropriate concentrations of nitrate or aspartate were used instead of TMAO.

ADDITIONAL REFERENCES:

Bailey S (1994) The Ccp4 Suite - Programs for Protein Crystallography. *Acta Crystallogr D* **50:** 760-763

Brunger AT, Adams PD, Clore GM, DeLano WL, Gros P, Grosse-Kunstleve RW, Jiang JS, Kuszewski J, Nilges M, Pannu NS, Read RJ, Rice LM, Simonson T, Warren GL (1998) Crystallography & NMR system: A new software suite for macromolecular structure determination. *Acta Crystallogr D* **54:** 905-921

Cheung J, Hendrickson WA (2009) Structural analysis of ligand stimulation of the histidine kinase NarX. *Structure* **17:** 190-201

Cowtan K (1994) *CCP4/ESF-EACBM Newsletter on Protein Crystallography* **31:** 34-38

Datta S, Costantino N, Court DL (2006) A set of recombineering plasmids for gram-negative bacteria. *Gene* **379:** 109-115

Hendrickson WA (1979) Transformations to Optimize the Superposition of Similar Structures. *Acta Crystallogr A* **35:** 158-163

Moore JO, Hendrickson WA (2009) Structural analysis of sensor domains from the TMAO-responsive histidine kinase receptor TorS. *Structure* **17:** 1195-1204

Neidhardt FC, Bloch PL, Smith DF (1974) Culture medium for enterobacteria. *J Bacteriol* **119:** 736-747

Otwinowski Z, Minor W (1997) Processing of X-ray diffraction data collected in oscillation mode. *Methods Enzymol* **276:** 307-326

Perrakis A, Morris R, Lamzin VS (1999) Automated protein model building combined with iterative structure refinement. *Nat Struct Biol* **6:** 458-463

Silhavy TJ, Berman ML, Enquist LW, (1984) *Experiments with gene fusions*, Cold Spring Harbor, N.Y.: Cold Spring Harbor Laboratory.

Terwilliger TC, Berendzen J (1999) Automated MAD and MIR structure solution. *Acta Crystallogr D* **55:** 849-861

Wang W, Malcolm BA (2002) Two-stage polymerase chain reaction protocol allowing introduction of multiple mutations, deletions, and insertions, using QuikChange site-directed mutagenesis. *Methods Mol Biol* **182:** 37-43

SUPPLEMENTARY TABLES:

Table S1, related to Table 1. Data collection statistics

Data Set	d_{min} (Å)	Wave-length (Å)	Number of Reflections	Average Redundancy	<I>/(σ(I))	Complete-ness (%)[a]	R_{merge} (%)[b]
Isopropanol $TorTS_S$	2.95	0.98009	262063	4.1	6.6 (1.8)	98.2 (98.7)	7.6 (47.2)
Se isopr'ol $TorTS_S$ λ1	3.5	0.97893 (Peak)	252302	3.5	8.5 (4.4)	92.3 (79.2)	11.0 (26.2)
Se isopr'ol $TorTS_S$ λ2	3.5	0.97924 (Edge)	293919	4.0	7.1 (3.7)	96.0 (86.0)	7.5 (24.7)
Se isopr'ol $TorTS_S$ λ3	3.5	0.97126 (Remote)	275748	3.8	5.0 (2.5)	93.9 (75.0)	10.2 (36.5)
TMAO-bound $TorTS_S$	3.1	0.90020	142440	5.2	11.2 (2.7)	95.9 (88.0)	1.1 (29.4)
Apo $TorTS_S$	2.8	0.97900	276208	6.5	11.9 (2.9)	99.9 (99.2)	14.1 (45.5)

[a] Values in the outermost shell are given in parentheses.

[b] $R_{merge} = (\Sigma |I_i - < I_i >|) / \Sigma |I_i|$, where I_i is the integrated intensity of a given reflection.

Table S2, related to Figure 3. Mutations and *in vivo f*unctional analyses

(A) TorT-TorS interface

Protein	V. para residue	E. coli mutant	β-Gal (U)	
			0mM	10mM
TorT	R325	R329D	22.3	196.9
TorT	R325	R329E	21.1	153.7
TorS	E257	E241R	17.4	381.7
TorS	E257	E241Q	16.4	439.5
TorS	D258	D242R	17.2	24.5
TorS	D258	D242N	25.6	300.8
TorS	D258	D242A	23.2	373.3
TorS	D258	D242S	18.5	275.2
TorS	D258	D242L	19.3	28.3
TorS	D258	D242V	25.0	83.9
Wild Type			22.6	336.5

(B) TorS-TorS interface between proximal domains

Protein	V. para residue	E. coli mutant	β-Gal (U)	
			0mM	10mM
TorS	P50	P37A	22.3	418.1
TorS	P50	P37S	18.3	23.0
TorS	R56	R43D	21.2	17.8
TorS	R56	R43E	19.8	19.9
TorS	R56	R43I	23.3	46.6
TorS	N311	S295D	22.6	73.7
TorS	N311	S295I	20.0	311.7
TorS	N311	S295R	18.8	294.5
TorS	D315	D299R	26.6	402.9
TorS	D315	D299N	15.7	372.9
TorS	D315	D299I	21.9	22.6
Wild Type			22.6	336.5

(C) Transmembrane interface mutation in ecTorS

Constructs are identified by labels that define segments in which interfacial residues were shifted in position. Predicted transmembrane segments are highlighted in gray, and interfacial segments subject to mutation are marked in red. Three-residue segments EAS and AQF were either deleted (Δ) or duplicated (+) in the associated mutation.

```
            WY18-2  STLWYLA NLRFI
            WY18-1  STLVWYA NLRFI
            WY18+1  STLVGLW YLRFI
            WY18+2  STLVGLV WYRFI                          Δ/+EAS
  1  MAGFALMALL TLTSTLVGWY NLRFISRVEK DNTQALIPTM NMARQLSEAS

                                          Δ/+AQF
251  ATTLTTVSQY SDLLALYQQD SEISNHLQTL AQNNIAQFAQ FSSEVSQLVD

             Y321-2   ASARY GLSLLLLG
             Y321-1   ASARG YLSLLLLG
             Y321+1   ASARG QLYLLLLG
             Y321+2   ASARG QLVYLLLG
301  TIELRNQHGL AHLEKASARG QYSLLLLGMV SLCALILILW RVVYRSVTRP

                                    WR339-2  LILWRV AVVYRSV
                                    WR339-1  LILIWR AVVYRSV
                                    WR339+1  LILILA WRVYRSV
                                    WR339+2  LILILA LWRYRSV
301  TIELRNQHGL AHLEKASARG QYSLLLLGMV SLCALILILW RVVYRSVTRP

              TM2-2   ASARY GLSLLLLGMV SLCALILWRV AVVYRSV
              TM2-1   ASARG YLSLLLLGMV SLCALILIWR AVVYRSV
              TM2+1   ASARG QLYLLLLGMV SLCALILILA WRVYRSV
              TM2+2   ASARG QLVYLLLGMV SLCALILILA LWRYRSV
301  TIELRNQHGL AHLEKASARG QYSLLLLGMV SLCALILILW RVVYRSVTRP
```

Mutant	[TMAO] 0mM	[TMAO] 10mM
WY18-2	40.1	143.7
WY18-1	112.6	148.8
Wild Type	0.9	190.2
WY18+1	1.3	34.6
WY18+2	6.0	191.7
W321-2	38.6	127.7
W321-1	35.7	139.6
Wild Type	0.9	190.2
W321+1	72.3	101.7
W321+2	8.9	176.2

WR339-2	38.6	125.4
WR339-1	1.0	149.1
Wild Type	0.9	190.2
WR339+1	72,3	91.0
WR339+2	8.9	29.5
TM2-2	115.6	126.1
TM2-1	76.3	307.4
Wild Type	0.9	190.2
TM2+1	105.0	496.2
TM2+2	9.7	75.4
Wild Type	0.9	190.2
ΔEAS	1.2	3.0
+EAS	1.2	19.0
ΔAQF	233.5	192.1
+AQF	1.5	1.7

(D) NarX-TorS chimera

Sequences of TorS (black), NarX (red), and the NarX-TorS fusion starting at the end of the second TM helix (highlighted in gray), and the first amphipathic segment of the HAMP domain (highlighted in yellow).

```
    TorS LILW -RVVYRSVTR- PLAEQTQALQRLLDGDI
    NarX TIIW --LRARLLQ-- PWRQLLAMASAVSHRDF
NarX_Tor TIIW --LRARLLQ-- PLAEQTQALQRLLDGDI
```

[NO_3] (mM)	β-Gal (U)
0	59.4
0.1	89.9
1	172.8
10	254.9
100	199.0

Table S3, related to Figure 4. Transformations of superposition

(A) Superpositions of quasi-symmetric mates in the apo TorT-TorS$_S$ structure

For each region (domain or subdomain), the Cα positions of the ' protomer was moved into optimal superposition with those of the " protomer through the transformation a rotation of chi and translation of tchi along the axis of rotation specified by orientation parameters phi and psi as defined by TOSS (Hendrickson, 1979).

Region:	TorT		Tower
	NTD	CTD	3_4
chi	174.58	177.32	179.79
tchi	-0.560	0.216	0.044
phi	162.89	164.33	-87.57
psi	51.28	52.96	0.57

Region:	Distal Domain				
	3456	3	4	5	6
chi	180.87	179.69	180.31	177.83	180.83
tchi	0.516	0.413	0.550	0.415	0.297
phi	159.57	160.04	160.10	159.64	159.9
psi	52.99	52.82	52.95	53.42	53.18

Region:	Proximal Domain					
	1236	126	1	2	3	6
chi	185	185.4	190.27	186.84	180.89	186.63
tchi	-0.556	-0.542	-0.685	-0.755	-0.304	-0.368
phi	158.55	158.61	157.66	158.16	159.19	159.23
psi	51.67	51.74	51.74	52.05	51.33	51.75

(B) Structural deviation after domain or subdomain superposition

Values are root-mean-squared deviations (RMSDs) between Cα positions within the indicated region. "Apo on TMAO" refers to the rigid-body superposition of the entire indicated TorS' + TorS" unit onto corresponding portions of the $TorS^T$ dimer.

Region:	TorT		Tower
	NTD	CTD	3_4
' onto "	0.435	0.443	0.418
' onto ^{T}	0.479	0.448	0.280
" onto ^{T}	0.407	0.423	0.343
Apo on TMAO	-	-	0.327

Region:	Distal				
	3456	3	4	5	6
' onto "	0.588	0.258	0.299	0.382	0.227
' onto ^{T}	0.315	0.222	0.243	0.283	0.321
" onto ^{T}	0.435	0.257	0.208	0.340	0.316
Apo on TMAO	0.388	-	-	-	-

Region:	Proximal					
	1236	126	1	2	3	6
' onto "	0.488	0.485	0.452	0.425	0.303	0.327
' onto ^{T}	0.563	0.571	0.445	0.534	0.369	0.500
" onto ^{T}	0.468	0.472	0.379	0.398	0.393	0.443
Apo on TMAO	0.902	0.904	-	-	-	-

(C) Conformational transition through TorS from apo to TMAO-bound states

For each region (domain or subdomain), the Cα positions of the designated apo helices were transformed by TOSS (Hendrickson, 1979). Here, having first superimposed the tower domains of the apo and TMAO-bound heterotetramers, elements of each apo distal bundle were superimposed onto corresponding TMAO-bound elements (see Figure 4E).

TorS' Tower Bundle to Distal Bundle					
Helices:	**3456**	**3**	**4**	**5**	**6**
chi	2.96	3.22	3	3.91	3.25
tchi	0.315	0.195	0.133	0.667	0.276
phi	-164.80	-155.27	-150.42	173.64	-169.91
psi	90.11	109.65	61.57	127.08	77.07
RMSD	0.333	0.222	0.243	0.3	0.3
TorS" Tower Bundle to Distal Bundle					
Helices:	**3456**	**3**	**4**	**5**	**6**
chi	3.57	3.14	3.39	3.98	3.08
tchi	0.002	-0.115	0.135	-0.167	0.131
phi	-151.92	-152.26	-158.93	-142.64	-149.44
psi	103.91	105.55	81.4	103.73	91.52
RMSD	0.435	0.257	0.208	0.323	0.341

(D) Conformational transition through TorS from apo to TMAO-bound states

For each region (domain or subdomain), the Cα positions of the designated apo helices were transformed by TOSS (Hendrickson, 1979). Here, having first superimposed the distal domains from apo and TMAO-bound structures, elements from the corresponding proximal bundles were superimposed (see Figure 4E).

TorS' Distal Bundle to Proximal Bundle						
Helices:	**1236**	**126**	**1**	**2**	**3**	**6**
chi	3.36	3.16	1.63	2.74	9.07	4.13
tchi	-0.226	-0.196	-0.067	-0.84	-0.233	0.009
phi	122.36	133.36	168.29	130.41	1.26	107.58
psi	170.84	166.94	68.89	86.76	167.47	172.35
RMSD	0.563	0.571	0.445	0.534	0.369	0.5
TorS" Distal Bundle to Proximal Bundle						
Helices:	**1236**	**126**	**1**	**2**	**3**	**6**
chi	8.44	8.56	10.24	7.79	9.39	10.55
tchi	-0.109	-0.090	-0.127	-0.519	-0.105	-0.091
phi	-95.88	-92.14	-95.51	-85.22	-112.28	-83.04
psi	153.08	154.46	156.68	140.42	155.18	161.59
RMSD	0.468	0.472	0.379	0.398	0.393	0.443

SUPPLEMENTARY FIGURES:

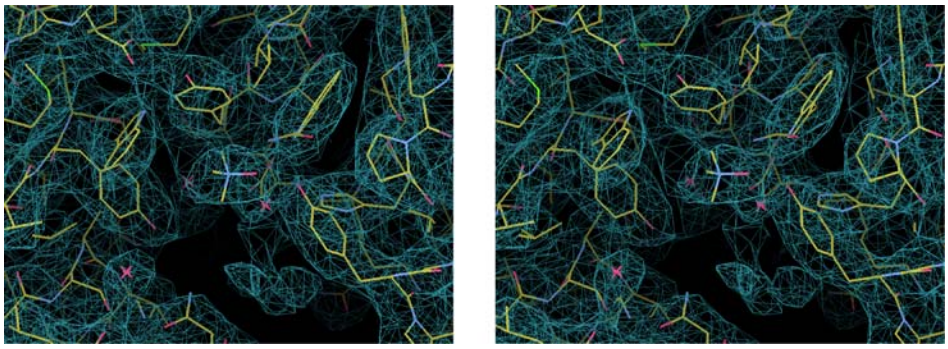

Figure S1, related to Table 1. Electron density distribution at the TMAO binding site of TorT in the heterotetrameric TorT(TMAO)-TorS$_S$ complex. The figure is drawn in stereo centered on a TMAO molecule in the same orientation as in Figure 3C. The final model is drawn with bonds colored by atom type: carbon (yellow), nitrogen (blue), oxygen (red) and sulfur (green). Contours from a 2Fo – Fc synthesis are drawn at the 1.5σ level.

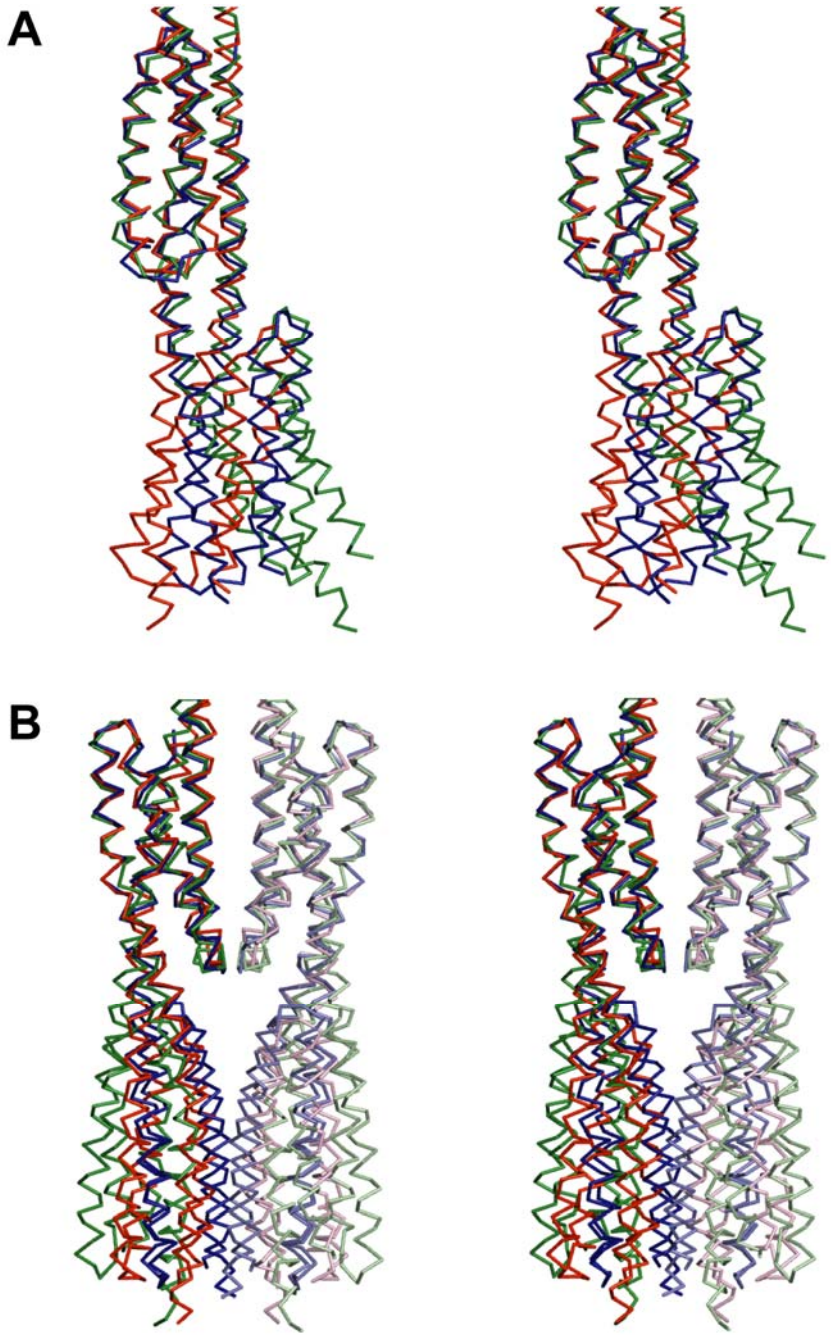

Figure S2, related to Figure Figure 1. Comparison of $TorS_S$ Structures in TorT-$TorS_S$ Complexes with Isolated $TorS_S$ Structures.

(A) Stereo diagram of the superposition of the distal domains of $TorS^T$ (red) with the monomeric structures of vp$TorS_S$ (blue) and ec$TorS_S$ (green). $TorS_S$ in all of the heterotetramer complexes is straightened even further from isolated ec$TorS_S$ (33.0-35.1°) than from isolated vp$TorS_S$ is from isolated ec$TorS_S$ (24.5°).

(B) Stereo diagram of the resulting dimeric structures generated when the distal domains from the monomeric structures of $vpTorS_S$,(blue) and $ecTorS_S$ (green) are independently superimposed on $TorS^T$ (red) and its symmetry mate (pink). The view here is related to A by a 90° rotation around the diad axis.

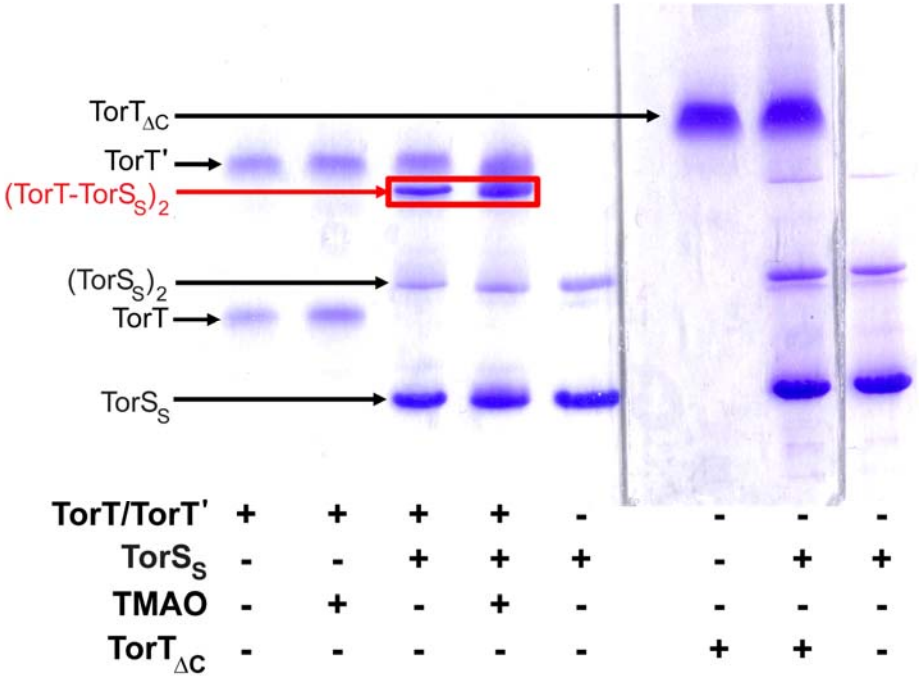

Figure S3, related to Figure 2. Native PAGE analysis of TorT-TorS$_S$ Interactions. Thrombin-cleaved TorT (TorT/TorT') and a recombinant, C-terminally truncated version (TorT$_{\Delta C}$) were run separately and also together with TorS$_S$. By SDS PAGE, thrombin-cleaved TorT is a mixture of intact TorT and a truncated version, identified here as TorT' and shown by N-terminal sequencing and mass spectrometry to be C-terminally truncated by ~21 residues, presumably at a thrombin site at Lys308. TorS$_S$ was in stoichiometric excess for the TorT experiments, which were run with TMAO as well as without TMAO, as indicated. Bands are assigned from uniqueness and expected mobilities based on charge, size and shape. TorS$_S$ was shown to dimerize with K_d = 282 μM; accordingly, both monomer and dimer bands are indicated. Gels were run at pH 8.8 where all His residues should be unprotonated and neutral, but Asp, Glu, Lys and Arg residues should be charged. Thereby, TorS$_S$, TorT and TorT$_{\Delta C}$ are expected to have net charges of -13, -5 and -1, respectively, in keeping with observed mobilities. The mobility of TorT' indicates a net charge of -2, contrary to what is expected for cleavage after Lys308 as suggested by mass spectrometry and as cloned for TorT$_{\Delta C}$. We do not understand the discrepancy, but neither TorT' nor TorT$_{\Delta C}$ binds to TorS$_S$ whereas TorT does. Essentially equivalent binding occurs whether TMAO is present or not.

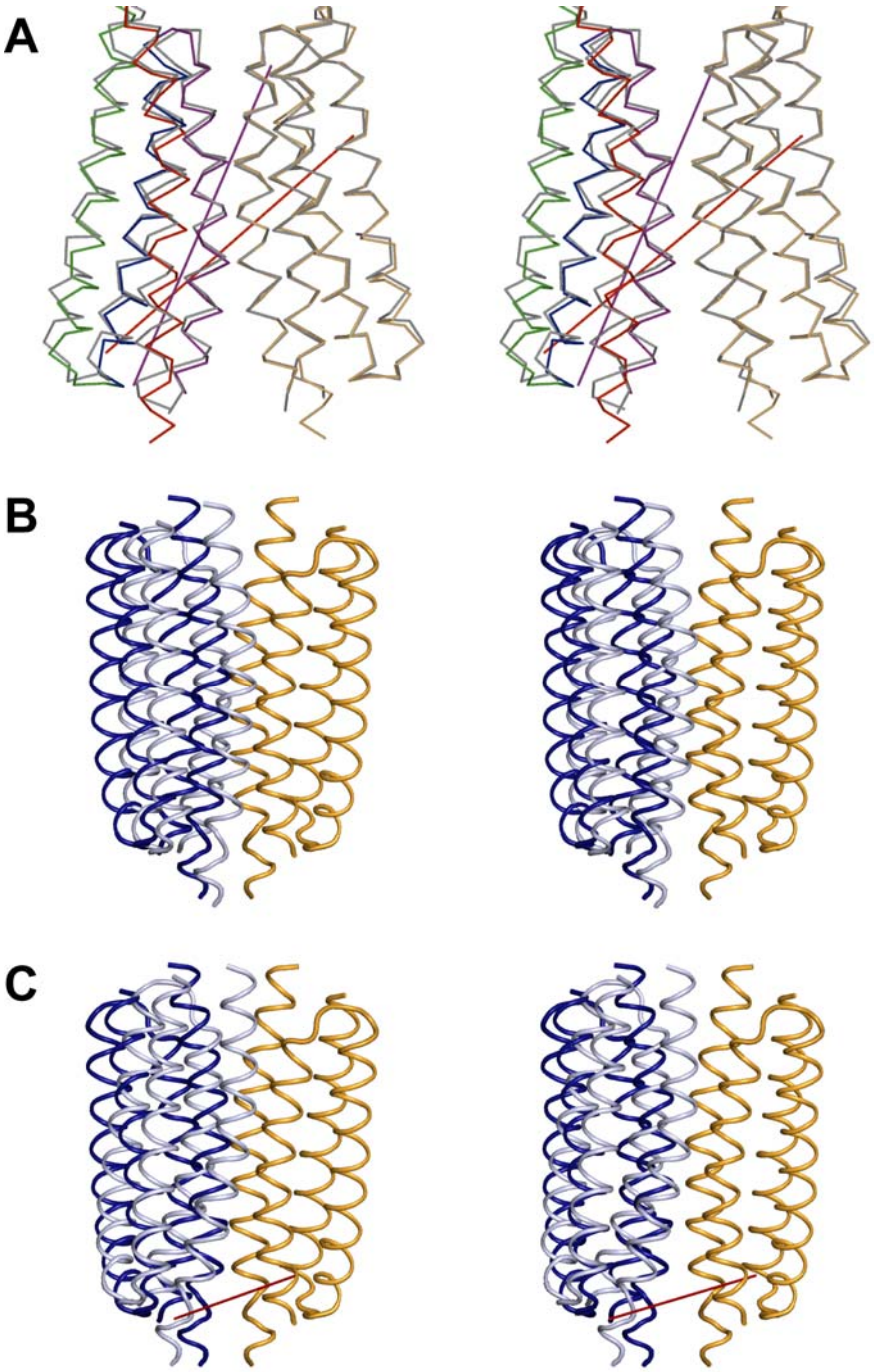

Figure S4, related to Figure 4. Proximal Domain Dimer Structures.

(A) Asymmetry-to-symmetry transition from apo $TorS_S$ to TMAO-bound $TorS_S$. Cα backbone drawings are shown in stereo with the $TorT^T$ diad axis vertical. The apo $TorS_S$ dimer (gray) is shown in stereo after superposition of the proximal bundle of TorS" onto a

corresponding bundle of $TorS^T$ (orange). The symmetry mate of $TorS^T$ is displayed with coloring such that α1 is purple, α2 is blue, α3 is green, and α6 is red. The axis of rotation necessary to superimpose helices α1 (purple) and α6 (red) of TorS' onto the corresponding residues of the $TorS^T$ symmetry mate are also shown.

(B) Comparison of TMAO-bound and 'NarX-like' TorS dimers. Worm drawings are shown in stereo as oriented in **(A)**. The natural $TorS^T$ dimer is colored; and one $TorS^T$ protomer (yellow) has been superimposed onto a NarX protomer (PDB id: 3EZH). The other $TorS^T$ protomer is then transformed from its natural position (blue) into its superposition (gray) onto the alternative NarX protomer. The axis of rotation (χ = 6.9° and t_χ = -0.5Å) that transforms the natural $TorS^T$ symmetry mate (blue) into that from the constructed NarX-like $TorS^T$ (gray) lies below the displayed structures.

(C) Comparison of TMAO-bound and 'Tar-like' TorS dimers. Worm drawings are shown in stereo with the natural $TorS^T$ dimer colored as in **(B)**. Similarly as in **(B)**, one protomer of natural $TorS^T$ (yellow) is as superimposed onto one subunit from Tar (chain A, PDB id: 1VLT), and its symmetry mate (blue) was transformed into its superposition (gray) onto the other Tar protomer (ligated subunit B) to form the 'Tar-like' $TorS^T$ dimer. The red rod shows the axis of rotation (χ = 13.8° and t_χ = 5.1Å) that transforms the natural $TorS^T$ symmetry mate (blue) into that from the constructed Tar-like $TorS^T$ (gray). The NarX and Tar sensor dimers are similar to one another[2], as is visually apparent here in comparing the NarX-like and Tar-like TorS dimers, but both differ appreciably from the natural $TorS^T$ dimer.

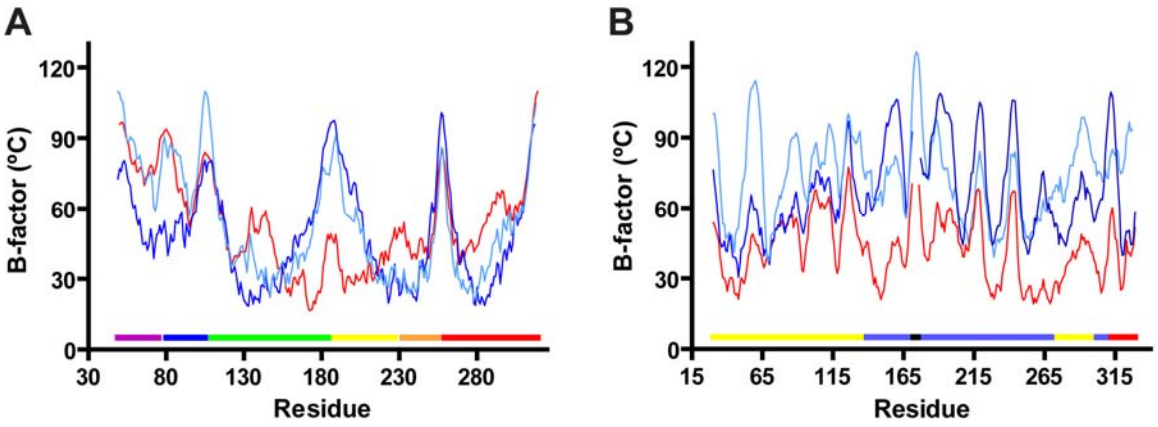

Figure S5, related to Figure 5. Atomic Mobility Profiles in TorT-TorS$_S$ Complexes.

(A) The C αB-factors are plotted vs. residue number for TorS^T (red) TorS' (dark blue) and TorS" (light blue). A colored bar along the x-axis indicates the location of the residues within α1 (purple), α2 (blue), α3 (green), α4 (yellow), α5 (orange), and α6 (red).

(B) The Cα B-factors are plotted vs. residue number for TorT^T.(red), TorT' (dark blue) and TorT" (light blue). A colored bar along the x-axis indicates the location of the residues within the NTD (yellow), the CTD (blue), the CTE (red), and the βF- α5 loop (black).